Title

Crystal Structure of a Family 80 Chitosanase From Mitsuaria Chitosanitabida

Author(s)

Yutaka Yorinaga, Takashi Kumasaka, Masaki Yamamoto, Kensaku Hamada, Makoto Kawamukai

Journal

FEBS Letters, Volume 591, Issue 3

Published

13 January 2017

URL

https://doi.org/10.1002/1873-3468.12557

Crystal structure of a family 80 chitosanase from *Mitsuaria chitosanitabida*

Yutaka Yorinaga,[1] Takashi Kumasaka,[2]* Masaki Yamamoto,[3] Kensaku Hamada,[4] and Makoto Kawamukai[1]*

[1]Department of Life Science and Biotechnology, Faculty of Life and Environmental Science, Shimane University, 1060 Nishikawatsu, Matsue 690-8504, Japan.
[2]Japan Synchrotron Radiation Research Institute (JASRI), Sayo, Hyogo 679-5198 Japan
[3]RIKEN SPring-8 Center, Sayo, Hyogo, 679-5148 Japan.
[4]X-ray Research Laboratory, Rigaku Co., Akishima, Tokyo, 196-8666 Japan.

*Corresponding authors:
Makoto Kawamukai: E-mail: kawamuka@life.shimane-u.ac.jp.
Telephone/Fax: 81-852-32-6583, Fax: 81-852-32-6092.
Takashi Kumasaka: E-mail: kumasaka@spring8.or.jp.

[1,2]These authors contributed equally to this work

Author Contributions: MK designed the project. YY was involved all experiments. TK, MY and KH contributed to structure determination and data interpretation. TK and MK wrote the manuscript. All authors read and approved the final manuscript.

The atomic coordinates and structure factors (PDB code 5B4S) have been deposited in the Protein Data Bank, Research Collaboratory for Structural Bioinformatics, Rutgers University, New Brunswick, NJ (http://www.rcsb.org/).

Abstract

Chitosanases belong to glycoside hydrolase families 5, 7, 8, 46, 75 and 80 and hydrolyse GlcN polymers produced by partial or full deacetylation of chitin. Herein, we determined the crystal structure of chitosanase from *Mitsuaria chitosanitabida* (McChoA) at 1.75 Å resolution, the first structure of a family 80 chitosanase. McChoA is a 34 kDa extracellular protein of 301 amino acids that fold into two (upper and lower) globular domains with an active site cleft between them. Key substrate-binding features are conserved with family 24 lysozymes and family 46 chitosanases. The distance between catalytic residues E41 and E61 (10.8 Å) indicates an inverting type mechanism. Uniquely, three disulphide bridges and the C-terminus might contribute to enzyme activity.

Key words: Chitosan, chitosanase, crystal structure, *Mitsuaria*

1. Introduction

Chitosan is a deacetylated product of chitin consisting of a polymer of N-acetyl glucosamine (GlcNac) that is generally thought to contain more than 50% glucosamine (GlcN). Chitosanases (EC3.2.1.132) hydrolyse chitosan into oligomers and dimers of GlcN; hence they are useful for producing chitooligosaccharides and GlcN for use in the food and pharmacological industries [1, 2]. Chitosanases belong to glycoside hydrolase (GH) families 5, 7, 8, 46, 75 and 80, based on the classification of Henrissat [3]. GH5, 7, and 8 chitosanases also possess other glycoside hydrolase activities such as cellulase and licheninase. Chitosanases have been found in many different microorganisms, including a few in plants [4]. The enzymatic properties and complete amino acid sequences of bacterial chitosanases have been reported from *Bacillus circulans* MH-K1 [5], *Streptomyces* sp. N174 [6], *Nocardioides* sp. N106 [7], *Nocardioides* sp. K-01, *Amycolatopsis* sp. CsO-2 [8], *Mitsuaria chitosanitabida* (formerly *Matsuebacter chitosanotabidus*) [9-11] and *Pseudomonas* sp. A-01 [12], and eukaryotic chitosanases from *Fusarium solani* [13] and *Aspergillus oryzae* [14] have also been reported. It is important to understand the substrate recognition and catalytic mechanisms of chitosanases based on their three-dimensional structures. Although crystal structures of chitinases from several species have been determined [15], structural information is only available for two families: family 46 (*Streptomyces* sp. N174, 1CHK [16]; *Bacillus circulans* MH-K1, 1QGI [17]; 2D05, K281P mutant [5]; *Streptomyces* sp. SirexAA-E, 4ILY; *Microbacterium* sp. OU01, 4OLT, inactive mutant with hexasaccharide; 4QWP, complex with digested substrates [18, 19]), and family 8 (*Bacillus* sp. K17 [20]). All of these are inverting type enzymes and are considered to act in a non-processive mode. In GH46, domain motion apparently results in an induced fit mechanism of substrate binding, as indicated by structural analysis of the *Microbacterium* sp. OU01 chitosanase complexed with hexaglucosamine ($(GlcN)_6$) [18, 19].

M. chitosanotabida, originally isolated as a chitosan degrading bacterium, belongs to the β-proteobacteria [21]. Chitosanase McChoA from *M. chitosanotabida* has been purified, and its gene cloned and sequenced [9], and functionally expressed in fission yeast [22]. The N-terminal 80 amino acid residues of McChoA are processed upon secretion. Two amino acids (Glu41 and Glu61) were identified as catalytic residues based on mutagenic analysis and catalytic activity measurements [23]. Chitosanases similar to McChoA are found in a variety of closely related species

isolated from natural environments [11]. A thermostable form of McChoA has been generated by random mutagenesis [10]. The accumulating knowledge suggests that this GH80 chitosanase has unique features. Previous purification and characterisation of McChoA is summarised in Table 1. McChoA is able to completely hydrolyse chitosan but not chitin or cellulose [9]. The gene encoding McChoA has been cloned and its amino acid sequence deduced. Full-length McChoA is synthesised as a 391 residue precursor, and the 80 N-terminal amino acids are removed during secretion [9].

In the present work, we determined the crystal structure of McChoA at 1.75 Å resolution, and explored this first structure of a GH80 chitosanase.

2. Materials and methods

2.1 Protein preparation

Recombinant ChoA from *M. chitosanotabida* was purified from *E. coli* expressing the gene encoding McChoA. Briefly, a ~1 kb DNA fragment encoding a 311 amino acid mature form of McChoA was cloned into the *Sph*I and *Hind*III sites of the pQE31 vector using standard procedures and primers TAGCATGCCGCCGCGGCGGGCGTGAT (to generate a *Sph*I site) and ATCCCGGGAAGCTTATTTGTATAGTTCATC (to generate a *Hind*III site) to amplify the *choA* gene by PCR. The resulting McChoA protein contains a hexa-histidine tag at the N-terminus. Native McChoA was expressed in *E. coli* JM109 cells, and purification of selenomethionine-substituted McChoA (Se-McChoA) was performed using *E. coli* B834 (DE3) harbouring pQE31-choA and pREP4 (*lacI* kan^r). *E. coli* B834 (DE3) cells were grown in minimal medium containing 50 µg/mL DL-SeMet and 50 µg/mL kanamycin and ampicillin to an optical density (OD_{600}) of 0.5. Expression of *choA* was induced with 1 mM isopropyl β-D-1-thiogalactopyranoside (IPTG), and culturing continued for a further 5 h at 37˚C. Cells were pelleted by centrifugation and disrupted by sonication. McChoA and Se-McChoA were purified using a Ni-NTA affinity column, and purified Se-McChoA at 20 mg/mL was used for crystallisation. Crystallisation of Se-McChoA was performed at 22°C by the sitting drop vapour diffusion method using 0.2 M ammonium sulphate, 25% (w/v) polyethylene glycol (PEG) 4000 and 0.1 M Na acetate (pH 5.6) as the precipitant. Crystals of Se-McChoA belong to the orthorhombic space group $P2_12_12_1$ with unit cell dimensions a = 51.9 Å, b = 56.4 Å and c = 207.1 Å.

2.2 Data collection and processing

X-ray diffraction data were collected from Se-McChoA crystals at beamline BL45XU of SPring-8 (Sayo, Hyogo, Japan) using radiation with a wavelength of 1.02 Å. X-ray diffraction experiments were performed under a cold N_2 gas stream (100 K) using a Rigaku R-AXIS V image plate detector. The structure was determined by MAD phasing as described previously [24]. The structural model was constructed with Arp/Warp [25] and refined with phenix.refine [26] following data re-processing using XDS [27]. There are two highly similar but independent ChoA molecules in the asymmetric unit with a root mean square deviation (rmsd) of 0.46 Å. Data collection and refinement statistics are listed in Table 2. Sequence alignment was performed with Clustal Omega [28], and figures were drawn using ESPript [29].

3. Results and discussion

3.1 Overall structure

The overall molecular structure of McChoA includes 12 α-helices and 5 β-strands (Figs. 1 and 2) that fold into upper and lower domains of comparable size; the upper domain of 153 amino acids spans residues 1–22 and 46–176 and includes helices α1–7 and strands β1–5; the lower domain of 158 amino acids spans residues 23–45 and 177–311 and includes helices α7–12. The longest helix, α7, forms the backbone that connects the two globular domains.

McChoA belongs to the GH80 group, which is grouped into the GH-I clan together with other inverting enzymes from GH24 (lysozymes) and GH46 (chitosanases). Although the sequence identity between McChoA and GH46 chitosanases whose structures have been determined is less than 20% (16.3% and 17.4% with *Streptomyces* sp. N174 and *Bacillus circulans* MH-K1 chitosanases, respectively), the overall assembly is similar, with all structures sharing a similar two-domain arrangement although some topological differences are apparent (Fig. 1). Conversely, GH8 chitosanase from *Bacillus* sp. K-17 shares only 11.1% sequence identity with McChoA, and has a very different topological assembly, forming a typical α6/α6 double barrel structure.

Due to the topological similarity with GH46 chitosanases, we were able to successfully superpose McChoA with the hexaglucosamine complex structure of

Microbacterium OU01 chitosanase (PDB ID: 4OLT; Figs. 3 and 4). Although each domain had to be aligned independently, no severe clashes resulted from the superposition, suggesting that the two domains of McChoA may be able to rotate almost 13°, as calculated by CCP4/DynDom [30]. This indicates that the domains of McChoA may close upon substrate binding. The mechanical hinges are formed from the loop regions between α1 and α2 (45–50) and α6 and α7 (158–163) that are analogous with residues 29–33 and 108–111 in OU01 chitosanase [19]. It is reasonable to assume a similar closed form of McChoA, even though insertions of two and six residues are present.

Another overall difference was the unique configuration of disulphide bonds in McChoA, which has six cysteines, all of which form disulphide bonds (Cys56-Cys151, Cys227-Cys235 and Cys260-Cys297; Fig. 2). One of them, Cys56-Cys151, was also observed in the *Bacillus circulans* MH-K1 chitosanase as Cys50-Cys124. Our previous mutational analysis showed that replacement of any of these cysteines results in the loss of catalytic activity [23]. The importance of these features is discussed in the following section.

3.2 Catalytic mechanism and substrate recognition

McChoA appears to catalyse an inverting hydrolysis reaction, based not only on the structural similarity with GH-I clan enzymes, but also the distance between the two catalytic residues (Glu41 and Glu61) determined in our previous work [23]. The active site cleft can be clearly seen, with Glu41 located on helix α1 of the lower domain, and Glu61 located on helix α3 of the upper domain (Fig. 2). The distance between oxygen atoms of Glu41 and Glu61 is ~10.8 Å. This value is similar to those in the apo structures of GH46 chitosanases, and consistent with the distance predicted for an inverting hydrolysis reaction [31]. By comparison, this distance is changed to 7.7 Å in the predicted closed McChoA structure.

Residues in the active site cleft are highly conserved with those of GH46 enzymes, implying a similar mechanism of substrate recognition. GH-I clan enzymes share an invariant core [32] comprising the region around one β-sheet consisting of β1, β2 and β3 in the upper domain, and the two helices (α1 and α8) that form the base of subsites in the lower domain. In the OU01 enzyme, Ser27 (corresponding to Gly43 in McChoA), Tyr37 (Tyr55), Arg45 (Arg70), Thr58 (Gly83), Asp60 (Asp84), His203 (no

equivalent in McChoA) and Asp235 (no equivalent in McChoA) form the -2, -1 and +1 subsites that are essential for substrate binding and catalysis [18]. Superposition of the structures indicated that Arg70 and Asp84 of McChoA are located in the -2 subsite (Fig. 4), consistent with our previous study in which mutation of these residues abolished catalytic activity [23].

By contrast, five distinct regions are visible in the primary sequence: (*i*) the loop between β1 and β2, which provides the catalytic base residue Glu61; (*ii*) the loop between α10 and α11 that forms the base of the kissing loops; (*iii*) the region containing β4 and β5 between α5 and α6; (*iv*) the loop connecting α8 and α9 that forms the -3 subsite in GH46 chitosanases; (*v*) α12 and its extended C-terminal region. The third of these regions is located far from the active site cleft and might only contribute to the integrity of the upper domain. Although the Asn142Ser mutation in this region increased enzyme activity [10], its relation to the structure remains unclear.

The first two regions described above form the edges of both globular domains in the active site cleft, and determine the dynamic and polymorphic character of GH46 chitosanases [33]. The lower domain loop between α9 and α10 (α10 and α11 in McChoA) is structurally different in the apo and substrate-bound forms in GH46 chitosanases [19]. Substrate binding presumably induces this variation that causes the loop to be flipped over the substrate or loop α2–β2 of the upper domain. This kissing structure might be maintained by a salt bridge between Arg45 and Glu200 in OU01 chitosanase (Fig. 4). In McChoA, Asp255 is one of three aspartates in the corresponding loop that may form a salt bridge with Arg70 in the upper domain. However, it is possible that the bulky loop β1–β2 containing a short helix may interfere with the flipping of the lower globular domain loop.

The last two regions might contribute to the -3 subsite. The extended C-terminal region is uniquely conserved in GH80 enzymes, and lies close to loop α8–α9. While the corresponding loop α7–α8 expands and forms the base of the -3 subsite in OU01 chitosanase, this region is compact and does not provide any subsites in McChoA. To compensate for this, the C-terminal extended chain spans across α11 and α10, and finally reaches and lies beside α9 to form this subsite (Figs. 2B and 4). At its C-terminal end, Gln311 is located close to the putative -3 subsite. Even though the electron density of its side chain is somewhat ambiguous, the backbone is clearly visible and supported

by hydrogen bonds between the NH group and the OG atom of Ser211. Moreover, the adjacent residue Trp310 is embedded in a hydrophobic cluster.

Interestingly, the C-terminal residue is limited to glutamine or asparagine in all known GH80 sequences. Although there is no direct evidence for its importance, we have a possible explanation. We previously reported that three nonsense mutants at the C-terminal region (Trp247*, Trp261*, Gln284*) abolished enzyme activity [23]. All of these mutants lack Gln311, and also Cys297. Since all six cysteines are needed for maximum catalytic activity as stated above, we conclude that they are essential for stabilising the proper folded structure. However, the Cys297Gly mutant did exhibit slight but significant catalytic activity, and the possibility that other disulphides may form cannot be excluded at this stage [23]. Although the -3 subsite is not considered to be essential for chitosan hydrolysis in GH46 [18, 19], the role of the C-terminal residue in GH80 should be investigated by mutagenesis and enzymatic assays.

Acknowledgments

We would like to thank Dr K Shimono for providing the materials used in this study. We also thank Dr T Nakagawa and various members of our laboratory for helpful discussion and experimental support. This work was partly supported by a Grant-in-Aid from the Ministry of Education, Culture, Sports, Science and Technology of Japan awarded to MK (#25660059).

References

1 Thadathil, N. and Velappan, S. P. (2014) Recent developments in chitosanase research and its biotechnological applications: a review. *Food Chem* **150**, 392-399.

2 Brzezinski, R. (2011) Uncoupling chitosanase production from chitosan. *Bioengineered Bugs* **2**, 226-229.

3 Cantarel, B. L., Coutinho, P. M., Rancurel, C., Bernard, T., Lombard, V. and Henrissat, B. (2009) The Carbohydrate-Active EnZymes database (CAZy): an expert resource for Glycogenomics. *Nucleic Acids Res* **37**, D233-238.

4 Hoell, I. A, Vaaje-Kolstad, G. and Eijsink, V. G. H. (2010) Structure and function of enzymes acting on chitin and chitosan. *Biotechnol Genet Eng Rev* **27**, 331-366.

5 Fukamizo, T., Amano, S., Yamaguchi, K., Yoshikawa, T., Katsumi, T., Saito, J., Suzuki, M., Miki, K., Nagata, Y. and Ando, A. (2005) *Bacillus circulans* MH-K1 chitosanase: amino acid residues responsible for substrate binding. *J Biochem* **138**, 563-569.

6 Fukamizo, T. and Brzezinski, R. (1997) Chitosanase from *Streptomyces* sp. strain N174: a comparative review of its structure and function. *Biochem Cell Biol* **75**, 687-696.

7 Masson, J. Y., Boucher, I., Neugebauer, W. A., Ramotar, D. and Brzezinski, R. (1995) A new chitosanase gene from a *Nocardioides* sp. is a third member of glycosyl hydrolase family 46. *Microbiology.* **141 (Pt 10)**, 2629-2635.

8 Saito, A., Ooya, T., Miyatsuchi, D., Fuchigami, H., Terakado, K., Nakayama, S. Y., Watanabe, T., Nagata, Y. and Ando, A. (2009) Molecular characterization and antifungal activity of a family 46 chitosanase from *Amycolatopsis* sp. CsO-2. *FEMS Microbiol Lett.* **293**, 79-84.

9 Park, J. K., Shimono, K., Ochiai, N., Shigeru, K., Kurita, M., Ohta, Y., Tanaka, K., Matsuda, H. and Kawamukai, M. (1999) Purification, characterization, and gene analysis of a chitosanase (ChoA) from *Matsuebacter chitosanotabidus* 3001. *J Bacteriol* **181**, 6642-9.

10 Yun, C., Matsuda, H. and Kawamukai, M. (2006) Directed evolution to enhance secretion efficiency and thermostability of chitosanase from *Mitsuaria chitosanitabid*a 3001. *Biosci Biotechnol Biochem* **70**, 559-563.

11 Yun, C., Amakata, D., Matsuo, Y., Matsuda, H. and Kawamukai, M. (2005) New chitosan-degrading strains that produce chitosanases similar to ChoA of *Mitsuaria*

chitosanitabida. *Appl Environ Microbiol* **71**, 5138-5144.

12 Ando, A., Saito, A., Arai, S., Usuda, S., Furuno, M., Kaneko, N., Shida, O. and Nagata, Y. (2008) Molecular characterization of a novel family-46 chitosanase from *Pseudomonas* sp. A-01. *Biosci Biotechnol Biochem* **72**, 2074-2081.

13 Liu, H., Zhang, B., Li, C. and Bao, X. (2010) Knock down of chitosanase expression in phytopathogenic fungus *Fusarium solan*i and its effect on pathogenicity. *Curr Genet* **56**, 275-281.

14 Zhang, X. Y., Dai, A. L., Kuroiwa, K., Kodaira, R., Nogawa, M., Shimosaka, M. and Okazaki, M. (2001) Cloning and characterization of a chitosanase gene from the koji mold *Aspergillus oryzae* strain IAM 2660. *Biosci Biotechnol Biochem* **65**, 977-581.

15 Fukamizo, T. (2000) Chitinolytic enzymes: catalysis, substrate binding, and their application. *Curr Protein Peptide Sci* **1**, 105-124.

16 Marcotte, E. M., Monzingo, A. F., Ernst, S. R., Brzezinski, R. and Robertus, J. D. (1996) X-ray structure of an anti-fungal chitosanase from *Streptomyces* N174. *Nat Struct Biol* **3**, 155-162.

17 Saito, J., Kita, A., Higuchi, Y., Nagata, Y., Ando, A. and Miki, K. (1999) Crystal structure of chitosanase from *Bacillus circulans* MH-K1 at 1.6-A resolution and its substrate recognition mechanism. *J Biol Chem* **274**, 30818-30825.

18 Lyu, Q., Wang, S., Xu, W., Han, B., Liu, W., Jones, D. N. and Liu, W. (2014) Structural insights into the substrate-binding mechanism for a novel chitosanase. *Biochem J* **461**, 335-345.

19 Lyu, Q., Shi, Y., Wang, S., Yang, Y., Han, B., Liu, W., Jones, D. N. and Liu, W. (2015) Structural and biochemical insights into the degradation mechanism of chitosan by chitosanase OU01. *Biochim Biophys Acta* **1850**, 1953-1961.

20 Adachi, W., Sakihama, Y., Shimizu, S., Sunami, T., Fukazawa, T., Suzuki, M., Yatsunami, R., Nakamura, S. and Takenaka, A. (2004) Crystal structure of family GH-8 chitosanase with subclass II specificity from *Bacillus* sp. K17. *J Mol Biol* **343**, 785-795.

21 Amakata, D., Matsuo, Y., Shimono, K., Park, J. K., Yun, C. S., Matsuda, H., Yokota, A. and Kawamukai, M. (2005) *Mitsuaria chitosanitabida* gen. nov., sp. nov., an aerobic, chitosanase-producing member of the '*Betaproteobacteria*', *Int J Syst Evol Microbiol* **55**, 1927-1932.

22 Shimono, K., Matsuda, H. and Kawamukai, M. (2002) Functional expression of chitinase and chitosanase, and their effects on morphologies in the yeast

Schizosaccharomyces pombe. *Biosci Biotechnol Biochem* **66**, 1143-1147.
23 Shimono, K., Shigeru, K., Tsuchiya, A., Itou, N., Ohta, Y., Tanaka, K., Nakagawa, T., Matsuda, H. and Kawamukai, M. (2002) Two glutamic acids in chitosanase A from *Matsuebacter chitosanotabidus* 3001 are the catalytically important residues. *J Biochem* **131**, 87-96.
24 Kumasaka, T., Yamamoto, M., Yamashita, E., Moriyama, H. and Ueki, T. (2002) Trichromatic concept optimizes MAD experiments in synchrotron X-ray crystallography. *Structure* **10**, 1205-1210.
25 Langer, G., Cohen, S.X., Lamzin, V.S. and Perrakis, A. (2008) Automated macromolecular model building for X-ray crystallography using ARP/ wARP version 7. *Nat Protoc* **3**, 1171-1179.
26 Afonine, P.V., Grosse-Kunstleve, R.W., Echols, N., Headd, J.J., Moriarty, N.W., Mustyakimov, M., Terwilliger, T.C., Urzhumtsev, A., Zwart, P.H., and Adams, P.D. (2012) Towards automated crystallographic structure refinement with phenix.refine. *Acta Cryst D* **68**, 352-367.
27 Kabsch, W. (2010) XDS. *Acta Cryst. D* **66**, 125-132.
28 Sievers, F., Wilm, A., Dineen, D., Gibson, T.J., Karplus, K., Li, W., Lopez, R., McWilliam, H., Remmert, M., Söding, J., Thompson, J.D., and Higgins, D.G. (2011) Fast, scalable generation of high-quality protein multiple sequence alignments using Clustal Omega. *Mol Syst Biol* **7**,539.
29 Robert, X. and Gouet, P. (2014) Deciphering key features in protein structures with the new ENDscript server. *Nucleic Acids Res* **42**(W1), W320-324.
30 Hayward, S., and Berendsen, H.J.C. (1998) Systematic Analysis of domain motions in proteins from conformational change; New results on citrate synthase and T4 lysozyme. *Proteins* **30**, 144-154.
31 Mhlongo, N. N., Skelton, A. A., Kruger, G., Soliman, M.E.S., and Williams, I.H. (2014) A critical survey of average distances between catalytic carboxyl groups in glycoside hydrolases. *Proteins* 8**2**, 1747-1755.
32 Monzingo, A.F., Marcott, E.M., Hart, P.J., Robertus, J.D. (1996) Chitinases, chitosanases, and lysozymes can be devided into procaryotic and eucaryotic families sharing a conserved core. *Nat Struct Biol* **3**, 133-140.
33 Viens, P., Lacombe-Harvey, M. E. and Brzezinski, R. (2015) Chitosanases from family 46 of glycoside hydrolases: from proteins to phenotypes. *Marine Drugs* **13**,

6566-6587.

Figure legends

Figure 1. Sequence alignment of McChoA with GH46 chitosanases. Amino acid sequences of *Mitsuaria chitosanitabida* ChoA (M. chit.), *Bacillus circulans* (1QGI), *Streptomyces* sp. N174 (1CHK), *Streptomyces* sp. SirexAA-E (4ILY) and *Microbacterium* sp. OU01 (4OLT) are indicated. The mature McChoA, which is generated after removal of the 80-residue N-terminal signal sequence, begins at Alanine 1. Amino acid residues that are identical in McChoA are indicated by white characters on a red background. Catalytic acid residues (Glu41 in McChoA) are indicated by a red star, and catalytic base residues in McChoA (Glu61) and GH46 chitosanases are indicated by a blue star and blue triangle, respectively. The secondary structures of McChoA and 4OLT are indicated above and below the alignment, respectively.

Figure 2. Three-dimensional structure of McChoA. The 12 α-helices are coloured red, and the 5 β-strands are coloured yellow. The N- and C-termini are also indicated. Disulphide bonds are shown in yellow stick representation and numbered using a smaller font size. The catalytic general acid (Glu41) and base (Glu61) are also shown.

Figure 3. Comparison with OU01 chitosanase. The enzyme-substrate model of McChoA was constructed by simply superposing each domain of McChoA onto the *Microbacterium* sp. OU10 chitosanase structure complexed with $(GlcNAc)_6$ as described. A, Structures of McChoA. The upper and lower domains of McChoA are coloured green and cyan, respectively. A transparent model of the lower domain indicates the original orientation in the crystal structure, as shown in Fig. 2B. B, Structure of OU10 chitosanase coloured magenta. $(GlcNAc)_6$ is shown in yellow stick representation in both figures.

Figure 4. Putative model of substrate binding. A close-up view of the superposed model shown in Fig. 3 coloured in the same way. Residues of McChoA described in the main text are labelled, and residues of OU01 chitosanase are coloured magenta. The figure is drawn as a parallel view stereo image.

Table 1 Characteristics of McChoA chitosanase from *Mitsuaria chitosanitabida* 3001

Molecular weight	33,613 (mature form) 41,742 (precursor form)
Length	311 aa (mature form) 391 aa (precursor form)
Optimum pH	5.0–6.0
Optimum temperature	30–40°C
Thermal stability	50°C (30% 1 hr)
pI	9.6
Preference of substrate	Chitosan (90% deacetylated) >Chitosan (100% deacetylated) >Colloidal Chitin

Table 2 X-ray data collection and structure determination statistics

	Se-Met ChoA
Space group	$P2_12_12_1$
Unit cell (Å) *a, b, c*	51.9, 56.4, 207.1
Wavelength (Å)	1.02
Resolution (Å)	43.66–1.75 (1.81–1.75)
R_{merge}	0.057 (0.139)
Completeness	0.993 (0.987)
Mean I / σ_I	23.7 (12.4)
$CC_{1/2}$	0.998 (0.988)
Number of observed reflections	446,719 (43,766)
Unique reflections	61,905 (6,048)
Number of atoms A / B / Wat	2,370 / 2,374 / 680
R_{work} / R_{free}	0.160 / 0.192
Rmsd for bonds	0.006
Rmsd for angles	1.04
Ramachandran favoured / outliers (%)	97.6 / 0
Clash score	1.6
Average B factor A / B / Wat	13.8 / 13.8 / 22.7

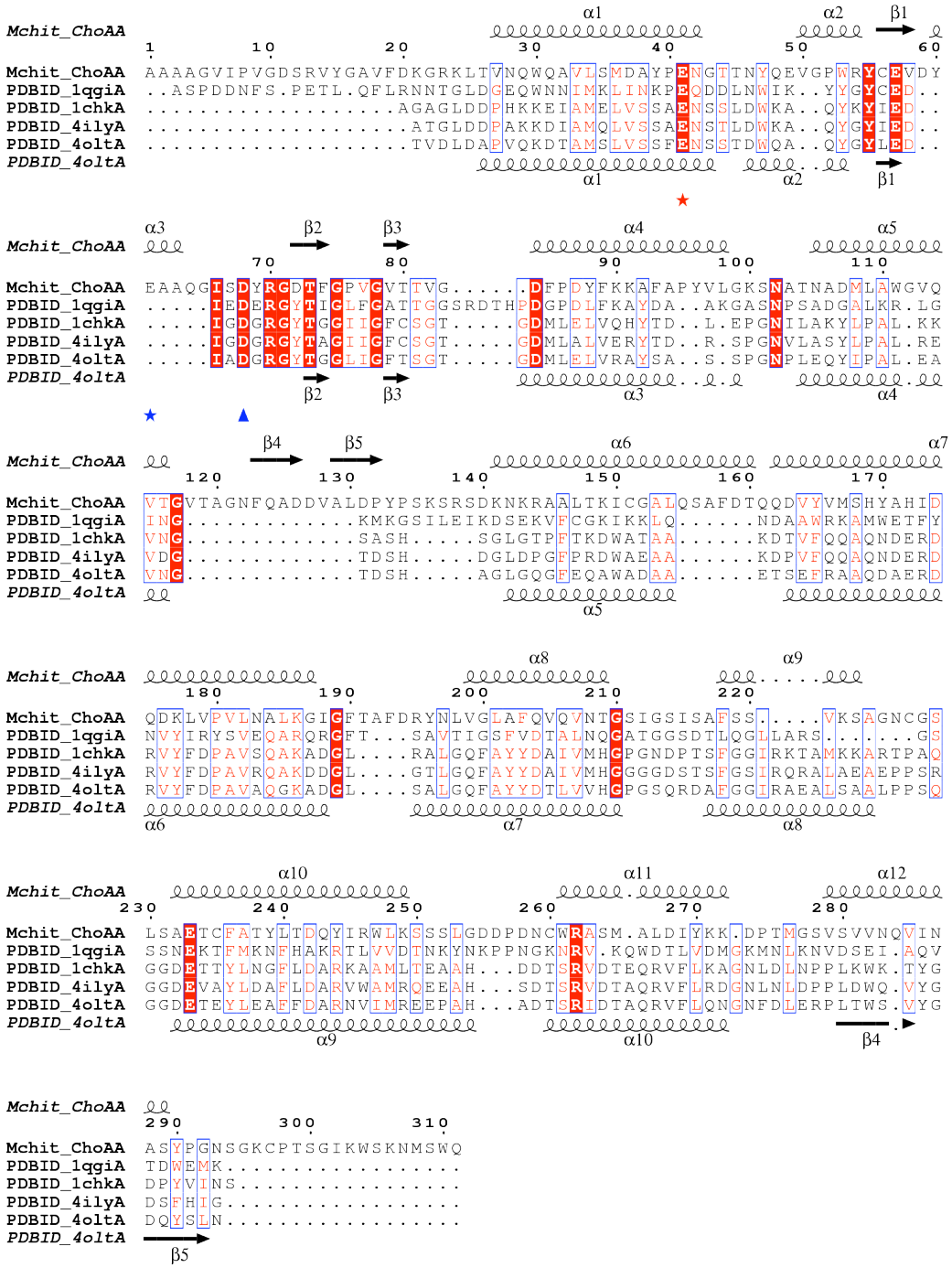
Mchit_ChoAA
PDBID_1qgiA
PDBID_1chkA
PDBID_4ilyA
PDBID_4oltA
PDBID_4oltA
α1
α2
β1
α3
β2
β3
α4
α5
β4
β5
α6
α7
α8
α9
α10
α11
α12
β5

Fig. 1

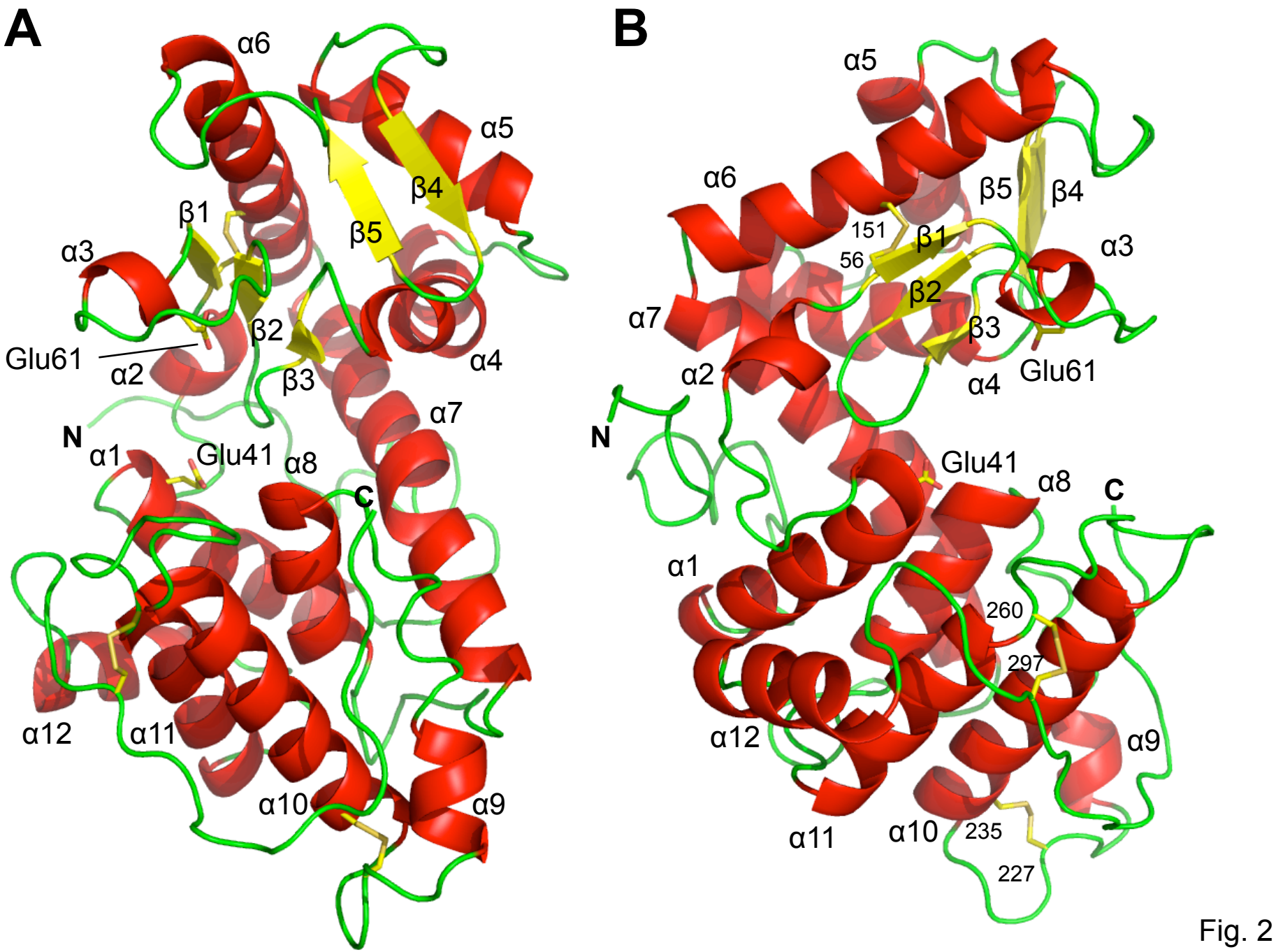
A
α6
α5
β4
β1
β5
α3
β2
Glu61
α2
α4
β3
α7
N
α1
Glu41
α8
C
α12
α11
α10
α9
B
α5
α6
β5
β4
151
β1
α3
56
β2
α7
β3
α2
α4
Glu61
N
Glu41
α8
C
α1
260
297
α12
α9
α11
α10
235
227

Fig. 2

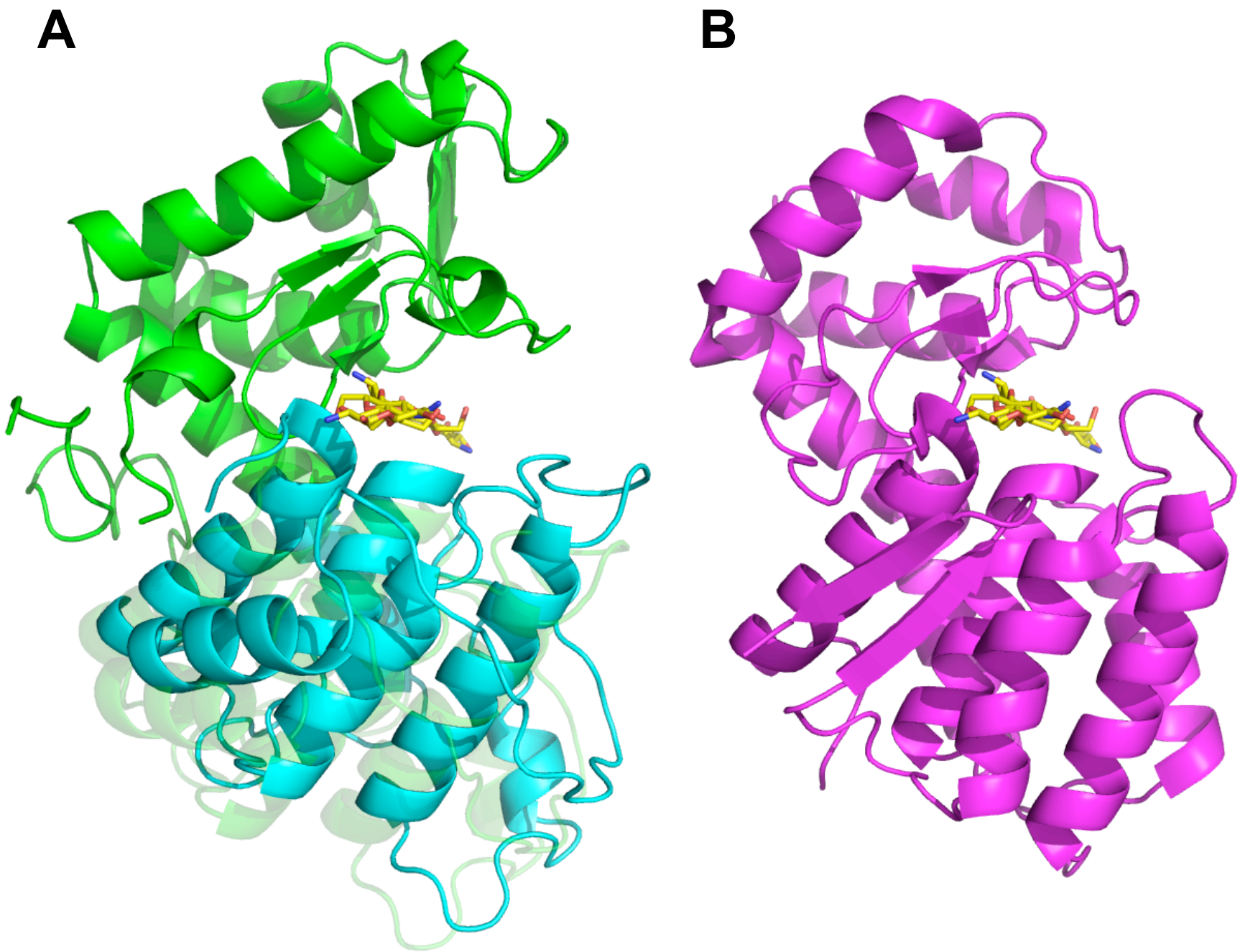

Fig. 3

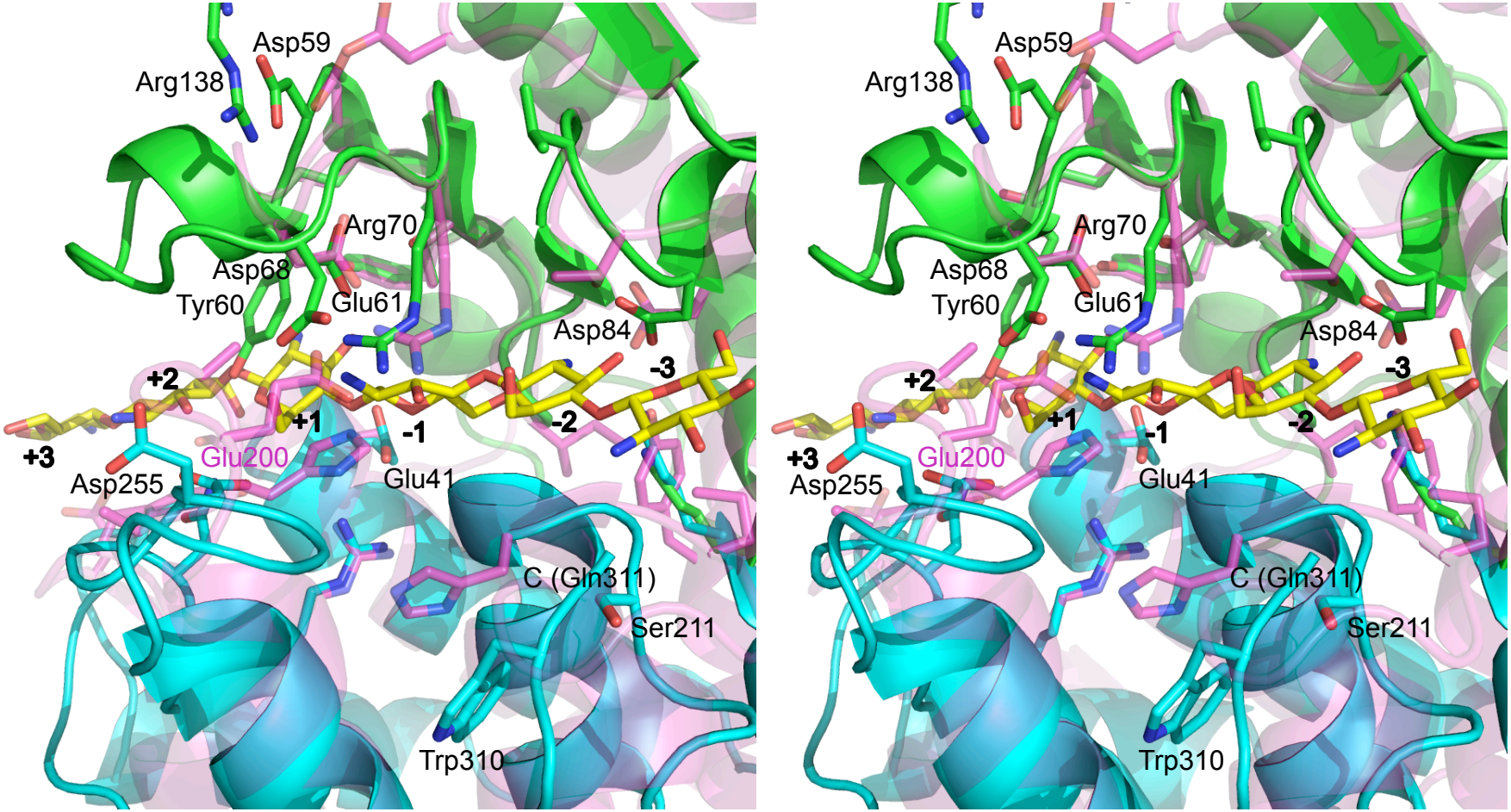
Asp59
Arg138
Arg70
Asp68
Tyr60
Glu61
Asp84
+2
+1
-1
-2
-3
+3
Glu200
Asp255
Glu41
C (Gln311)
Ser211
Trp310
Asp59
Arg138
Arg70
Asp68
Tyr60
Glu61
Asp84
+2
+1
-1
-2
-3
+3
Glu200
Asp255
Glu41
C (Gln311)
Ser211
Trp310

Fig. 4